J. Membrane Biol. 131, 245–256 (1993)

The Journal of
Membrane Biology


# Divalent Effects on cGMP-Activated Currents in Excised Patches from Amphibian Photoreceptors

Jacqueline C. Tanaka† and Roy E. Furman‡

†Department of Biochemistry and Biophysics, University of Pennsylvania Medical School, Philadelphia, Pennsylvania 19104-6089, and ‡Scientific Software Tools, Inc., Penn State Technology Development Center, Malvern, Pennsylvania 19355

**Summary.** The light-sensitive current in photoreceptors is conducted by a single class of ion channels gated by the binding of multiple molecules of cytoplasmic cGMP. Both Na and Ca ions enter the outer segment through this channel and Ca behaves as a blocking ion, greatly reducing the influx of Na. Because intracellular Ca functions as the cytosolic messenger for light adaptation, and this channel is the major entry point for Ca into the outer segment, we seek a better understanding of the selectivity properties of the channel and how they affect intracellular Ca levels. In these studies, we added divalent cations to the cytoplasmic face of an excised patch at constant, symmetrical [Na]. Our results suggest a novel high-affinity divalent binding site at the internal face of the channel. At constant low levels of cGMP, the addition of 10–100 nM cytoplasmic Ca or Mg attenuated the current 5- to 10-fold. There is also a low-affinity site, midway through the transmembrane field; saturation of this site reduces the divalent-free current ~100-fold. The presence of a high-affinity cytoplasmic site raises the question of whether Ca regulates the photoreceptor current through a direct interaction with the channel perhaps altering the channel selectivity or kinetics.

**Key Words** vision · phototransduction · nucleotide-gated channel · divalent block · macroscopic current recording

## Abbreviations

cGMP, 3-′5′-cyclic guanosine mono-phosphate; *I-V*, current-voltage relation; $Ca_i$, cytoplasmic $Ca^{2+}$ concentration; $I_{Na}$, sodium current; OS, outer segment. Elemental symbols such as Na and Ca were used throughout the manuscript to indicate the appropriate ions such as $Na^+$ and $Ca^{2+}$.

## Introduction

Light-sensitive current in the retinal photoreceptor outer segment (OS) is thought to be carried through a single class of ion channels. The opening probability of a channel is governed by a cooperative binding reaction involving three or more cytoplasmic cGMP molecules (reviewed by Liebman, Parker and Dratz, 1987 and Yau and Baylor, 1989). A dynamic interplay between cGMP synthesis and hydrolysis results in changes in cytoplasmic cGMP levels which, in turn, regulate the OS membrane potential. The nucleotide, therefore, links the photochemical reactions on the disc membrane to the voltage signaling across the plasmalemma.

The light-sensitive current, conducted through the nucleotide-activated channels, is carried by both Na and Ca ions and relevant experiments are discussed in the review by Yau and Baylor (1989). Since Ca has an important role as the intracellular second messenger for light adaptation and the cGMP-activated channel is the primary entry path for Ca in the OS (*see* Yau, 1991 and references listed within), an important biophysical goal is to understand how the cGMP-activated channel processes both ions and what factors modulate the fraction of light-sensitive current carried by Ca. Electrophysiological approaches, particularly current recordings from excised OS patches, provide a preparation in which voltage, cGMP levels and the ionic environment are under the control of the investigator (Hamill et al., 1981). Using this technique, a great deal has been learned about channel activation and monovalent ion selectivity in the absence of divalent cations (Karpen et al., 1988; Tanaka, Eccleston & Furman, 1989; Furman & Tanaka, 1990; Menini, 1990, and references listed within these papers).

An obvious limitation of electrical recordings, however, is that the movement of Na and Ca are indistinguishable, restricting the type of questions one can address about the Na : Ca selectivity of the channel. In addition, Ca is a potent blocker of Na movement through the channel reducing the current magnitude 10- to 200-fold when both Na and Ca are present. Currents in pure Ca solutions are also small, and it has not been possible to measure current reversal potentials under divalent bionic conditions

to estimate the relative permeability of the channel (*unpublished results;* Colomartino, Menini & Torre, 1991).

To better understand the interaction of Ca with the channel, we took advantage of the divalent block and treated the divalent as an inhibitor of the sodium current. Ca was added to the cytoplasmic face of a patch at constant, symmetrical Na concentrations and the macroscopic currents were examined at 20 and 200 $\mu$M cGMP. We found evidence for at least two Ca binding sites; one was a high affinity site which effected changes in the current at concentrations as low as 10 nM Ca and the other, with a $K_{0.5}$ in the mM range, produced a strong, voltage-dependent block. The effects at low Ca levels were more apparent when the cGMP concentration was 20 $\mu$M cGMP, which is near the $K_{0.5}$ for channel activation.

Preliminary reports of this work have been published (Tanaka & Furman, 1990; Su, Furman and Tanaka, 1991).

## Materials and Methods

### Materials

EGTA, HEPES, HEDTA, NaCl and 3′5′ guanosine cyclic monophosphate (cGMP) were obtained from Sigma Chemical; EDTA was obtained from Baker and $MgCl_2$, $CaCl_2$ were obtained from Fisher Scientific.

### Preparation

Full details of the preparation have been presented (Furman & Tanaka, 1990). Retinas were dissected under red light from dark-adapted *Rana pipiens* in a Ringer solution containing (mM) 112 NaCl, 1.9 KCl, 1.1 $CaCl_2$, 5 HEPES, pH 7.4, 1.6 $MgCl_2$ and 5 glucose. The retinas were stored in cold Ringer in a dark container; small aliquots (5 $\mu$l) of dissociated photoreceptors were layered onto the bottom of the chamber. The addition of 0.5% Percoll to the Ringer solution seemed to promote settling of the rods onto the chamber floor. After the cells settled to the floor, solution was continuously flowed into the chamber through a small S-shaped delivery tube. All experiments were done at room temperature and in room light.

### Current Recording

Complete details of the patch electrodes and the electronics have been previously reported (Furman & Tanaka, 1988, 1990). Corning 0010 glass was used to pull electrodes with tip resistances of 10–20 M$\Omega$. The electrodes were filled with a solution containing (mM) 120 NaCl, 1 EDTA, 1 EGTA, 5 HEPES/Na at 7.2 pH (Solution A).

The electrodes were connected to the headstage of a Dagan 8900 patch-clamp amplifier through a Ag/AgCl wire which was held inside the electrode by a 120-mM KCl agar bridge. Similar bridges were used for both the ground electrode and a bath reference amplifier that compensated for liquid-junction potentials.

Once a tight seal was obtained (1–5 G$\Omega$), the electrode was moved into the solution stream of the S-shaped inflow tube, providing sharp solution boundaries as the solutions were changed. This design minimized the equilibration time of each solution switch and was necessary to permit recordings from 12 solutions with minimal changes in the seal properties.

A 700-msec linear voltage ramp from −90 mV to 90 mV was applied to an excised membrane patch as previously described (Tanaka et al., 1989) and the current was low-pass filtered at 1 kHz (eight-pole Bessel, Frequency Devices, Haverhill, MA). Currents were simultaneously displayed on storage oscilloscope and stored to hard disc at 5 kHz by a 12-bit A/D (Labmaster, Scientific Solutions, Solon, OH).

The leak current was measured in the absence of nucleotide with symmetrical solutions across the patch. cGMP-activated currents were measured after ~1-min exposure to a solution containing cGMP. The control current was digitally subtracted from the activated current during analysis as detailed in Furman and Tanaka (1990), and all results are presented as net cGMP-activated currents. Currents are displayed in the physiological convention where negative potentials generate inward membrane currents from pipette to bath.

### Controls

To record currents in a single patch as divalent ion concentrations were explored from $10^{-9}$ M to $10^{-2}$ M, we first determined that the seal resistance in the absence of cGMP showed little change from $10^{-9}$ M to 1 mM Ca or Mg. We then routinely subtracted the leak current recorded in Solution A, in the absence of nucleotide, from all cGMP-activated traces with divalent concentrations less than 1 mM. For solutions containing 1 mM or 10 mM Ca or Mg, the leak current was measured with the divalent cation, in the absence of cGMP, and subtracted from the current with cGMP.

The patches we used for analysis were stable, retained their responsiveness to cGMP and were reproducible with multiple application of the same concentration of divalent cations. The results were independent of the order of presentation of the solutions. Exposure of the patch to high concentrations of divalent cations for long times (the average exposure time was 1–2 min) often resulted in large increases in the current, especially at low concentrations of cGMP. Some of this was due to slowly reversible changes in the seal resistance and some may have been due to changes in the channel sensitivity to cGMP (Kantrowitz-Gordon & Zimmerman, 1991). We routinely kept the exposure of the patch to high divalents as brief as possible and returned to the control solution to be sure that the maximal response to cGMP was unchanged. If the control current attenuated during the application of the solutions, we repeated the run: if the patch lost its responsiveness, we rejected it for analysis.

### Divalent Solutions

For most of the experiments reported in this paper, the bath contained Solution A (120 mM NaCl, 5 mM HEPES, pH 7.2 and 1 mM NaEGTA and 1 mM NaEDTA). The total divalent required to obtain the desired free concentration with 1 mM of both EDTA and EGTA present was calculated using a computer program, Max Chelator 3.1, which was generously distributed by Chris

Patton, Hopkins Marine Station, Pacific Grove, CA. The stability constants from Martell and Smith (1974) for EDTA binding Ca were 10.69 and 3.18 and for Mg were 8.79 and 3.85 at 0.12 N salt and 20°C and from Fabiato and Fabiato (1979) for EGTA were 10.72 and 5.33 for Ca and 5.21 and 3.37 for Mg. HEDTA alone was used to buffer Ca at $10^{-6}$ and $10^{-5}$ M. The total divalent metal added with 1 mM of EDTA and 1 mM EGTA is given in parentheses following the free concentration: $10^{-9}$ M Ca ($4.6 \times 10^{-5}$ M); $10^{-8}$ M Ca ($3.5 \times 10^{-4}$ M); $10^{-7}$ M Ca ($1.2 \times 10^{-3}$ M). At $10^{-6}$ M Ca, 1 mM HEDTA was used to buffer the Ca and $2.88 \times 10^{-4}$ M Ca was added; at $10^{-5}$ M Ca, $8.11 \times 10^{-4}$ M Ca was added. For the Mg solutions with 1 mM EDTA and 1 mM EGTA the free concentrations used the following total amounts of metal; $10^{-9}$ M Mg ($5.3 \times 10^{-7}$ M); $10^{-8}$ M Mg ($5.2 \times 10^{-6}$ M); $10^{-7}$ M Mg ($5.0 \times 10^{-5}$ M); $10^{-6}$ M Mg ($3.5 \times 10^{-4}$ M); and $10^{-5}$ M Mg ($8.5 \times 10^{-4}$ M). At higher concentrations, the free divalent was equal to total divalent in the absence of chelator. In our initial experiments, we verified with a Ca electrode that the measured level of free Ca in the solutions was equal to that calculated over the range of $10^{-7}$ M to $10^{-5}$ M Ca.

### Calculation of Fraction Block

The fraction of current blocked by divalents was determined by first averaging the net cGMP current over 1-mV neighborhoods at 10-mV intervals from −90 mV to 90 mV. The averaged control current in the absence of divalent cations, $I_{max}$, and the averaged current in the presence of Ca or Mg, $I_{test}$, were used to estimate

$$\text{Fraction Block } (F_b) = (I_{max} - I_{test})/I_{max}.$$

$$\text{Fraction Unblocked } (F_{ub}) = 1 - F_b$$

### Three-Dimensional Plots

Currents were collected during application of linear voltage ramps from −90 mV to 90 mV and then from 90 to −90 mV. The currents, consisting of 4676 a/d points, were digitally averaged from each ramp and stored to disc as a single ramp of 2338 a/d current values. Previously, we determined that the ramp *I-V* was equivalent to the steady-state *I-V* because currents averaged during the last 50 msec of 100-msec voltage steps coincided with the continuous *I-V* generated from the slow, 700-msec, voltage ramp (*see* Fig. 1, Furman & Tanaka, 1990).

In order to appreciate the changes in the *I-V* relations as the concentration of divalent cations was altered, three-dimensional plots were constructed from the *I-V* relations at each divalent concentration. For each patch, the currents were averaged in 4-mV neighborhoods every 10 mV and the averaged current values, voltages and divalent concentrations were entered into the Grid program in Surfer® (Golden Software, Golden, CO). The minimum curvature smoothing function was then used to develop a grid. This process first calculates initial values for the grid elements based on the data and then repeatedly applies the minimization algorithm (Briggs, 1974) to the surface. The grid is recalculated at progressive iterations until successive changes in the values of the elements are within a user-specified maximum absolute error. The three-dimensional surface was then constructed from the Grid using the Surfer® program. For most of the plots, a 300° angle of rotation about the z axis was used with an orthographic perspective and a 30° tilt after rotation to permit viewing of the entire data surface. Z-axis scaling factors and x : y ratios were adjusted for each plot based on the current magnitude to maintain a similar visual perspective among the variables.

## Results

In these studies, Ca and Mg were treated as classical inhibitors of the sodium transport through the cGMP-activated channel in order to develop a better understanding of the nature of the divalent interactions with the channel. The experimental protocol maintained a constant [Na] on both sides of an excised patch while Ca or Mg was varied at the cytoplasmic face. The first set of experiments were done with saturating levels of cGMP; the second set used levels of 20 μM cGMP, near the $K_{0.5}$ for current activation.

### Changes in the *I-V* Relations at Saturating [cGMP] as a Function of Increasing Calcium

The current activated by 200 μM cGMP was recorded in response to a linear voltage ramp at increasing Ca concentrations; results from a typical experiment are shown in Fig. 1*A*. Inward currents at hyperpolarizing potentials can be conceptualized as Na movement from the extracellular side of the membrane (pipette) to the cytoplasmic side (bath) in the presence of a cytoplasmic divalent blocker. Outward currents are more complex as they transport ions under varying ionic conditions from the cytoplasmic side (bath) into the pipette.

In the absence of divalent cations, the Na current-voltage (*I-V*) curve shows a slight outward rectification due to weakly voltage-dependent channel opening transitions at saturating concentrations of cGMP (*see* discussion, Tanaka et al., 1989). At low levels of free Ca, the currents are similar and difficult to distinguish in this graphical presentation. Above $10^{-5}$ M Ca, the currents in both directions are attenuated as a function of increasing [Ca]. Above 1 mM Ca, the inward currents change shape such that the shallow slope at potentials between zero and −30 mV becomes significantly steeper with more hyperpolarization. This profile is consistent with a voltage-relieved Ca block produced by Ca entering into the channel from the cytoplasmic side, against the thermodynamic gradient, and briefly impeding the net inward Na flux. As the hyperpolarization increases, the thermodynamic gradient becomes steeper and the entry rate for Ca ions moving uphill into the channel decreases.

Outward currents reflect the movement of both Na and Ca through the channel from the bath to the pipette. At Ca levels of $\geq 10^{-5}$ M, attenuation of

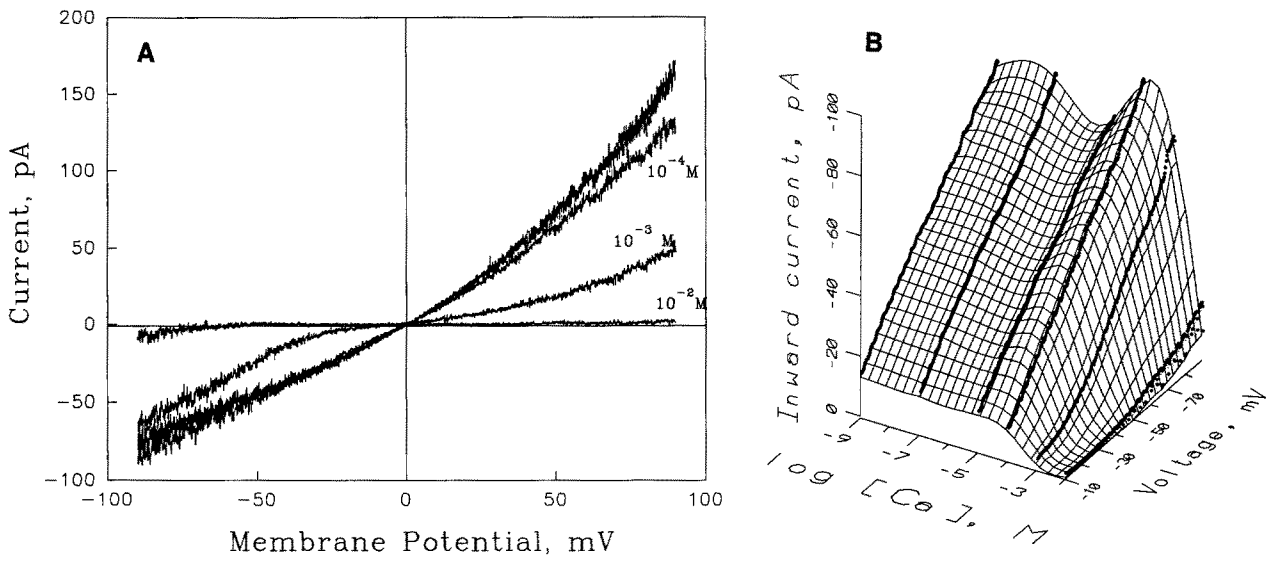


**Fig. 1.** (*A*) Current-voltage (*I-V*) relations at 200 $\mu$M cGMP as cytoplasmic [Ca] is increased. Macroscopic *I-V* relations were recorded from inside/out membrane patches excised from *Rana pipiens* rod outer segments by applying a 700-msec linear voltage ramp from −90 to 90 mV. Control *I-V*'s in the absence of cGMP were subtracted as described in Materials and Methods. The largest trace was the *I-V* recorded with symmetrical Solution A on both sides of the membrane in the presence of 200 $\mu$M cGMP on the cytoplasmic face (*see* Furman and Tanaka, 1990). *I-V*'s were recorded as $[Ca]_i$ was increased in the bath (cytoplasmic face) at constant 120 mM NaCl. Traces shown were $10^{-7}$, $10^{-5}$, $10^{-4}$, $10^{-3}$, and $10^{-2}$ M Ca. The traces at concentrations less than $10^{-4}$ M, overlay each other in this graphical presentation. The inward current at $10^{-4}$ M $Ca_i$ overlaps the first three traces, but the outward current shows considerable attenuation. The smallest currents were recorded in 1 and 10 mM Ca and show progressive block. Both inward and outward currents are >90% attenuated at 10 mM Ca in the bath. Patch 9322c4. (*B*) Three-dimensional surface showing current, voltage and Ca concentration at 200 $\mu$M cGMP. Net cGMP inward currents and voltages at varying [Ca] were entered into Surfer®, a three-dimensional plotting routine, and used to calculate a three-dimensional grid. A minimum curvature routine in the Surfer® program was used to develop the surface (*see* Materials and Methods), on which the actual data are plotted. By following the top of the surface from left to right, we see changes in the current as Ca is raised from 1 nM to 10 mM.

the outward current is seen without a change in curvature of the *I-V*. This feature might be expected if Ca is permeant but has a smaller conductance than Na.

Previous experiments directed us to look for a high affinity divalent binding site in addition to the prominent one at ~1 mM. In planar bilayers containing cGMP-activated channels (Tanaka et al., 1987), large increases in the currents were seen when divalent levels were decreased below ~100 nM. To determine whether these changes could be seen in in situ currents, we explored a large range of divalent concentrations. Although not apparent in Fig. 1*A*, we consistently saw subtle, but reproducible and reversible, current changes at very low $[Ca]_i$. To better visualize these data, three-dimensional surfaces of current *vs.* voltage *vs.* divalent concentration were constructed. The current *vs.* voltage relations in Fig. 1*A* were used to form the surface shown in Fig. 1*B*. Traditional current *vs.* concentration relations are displayed in the x-y plane and voltage is plotted in the z axis. The top edge of the surface in Fig. 1*B*, furthest from the eye, shows the inward current *vs.* [Ca] at −90 mV. Following the direction of increasing Ca concentration (left to right), the current displays complex behavior with several peaks and valleys apparent.

The three-dimensional surface shows clear and strong block of inward currents by cytoplasmic Ca in the mM range. The midpoint of block appears to be between 1 and 10 mM Ca at −90 mV. The voltage dependence of this block is appreciated by following the curvature of the current *vs.* voltage lines at high Ca concentrations. In contrast, the changes in current seen at the low concentrations of Ca show little curvature suggesting that these effects are relatively voltage independent.

The data shown in Fig. 1 are consistent with reports by Colomartino et al. (1991) and Zimmerman and Baylor (1992) of divalent block of the inward current by mM concentrations of divalent cations. In addition to this site, our data also suggest the existence of a much higher affinity binding site producing changes in the currents at very low levels of Ca.

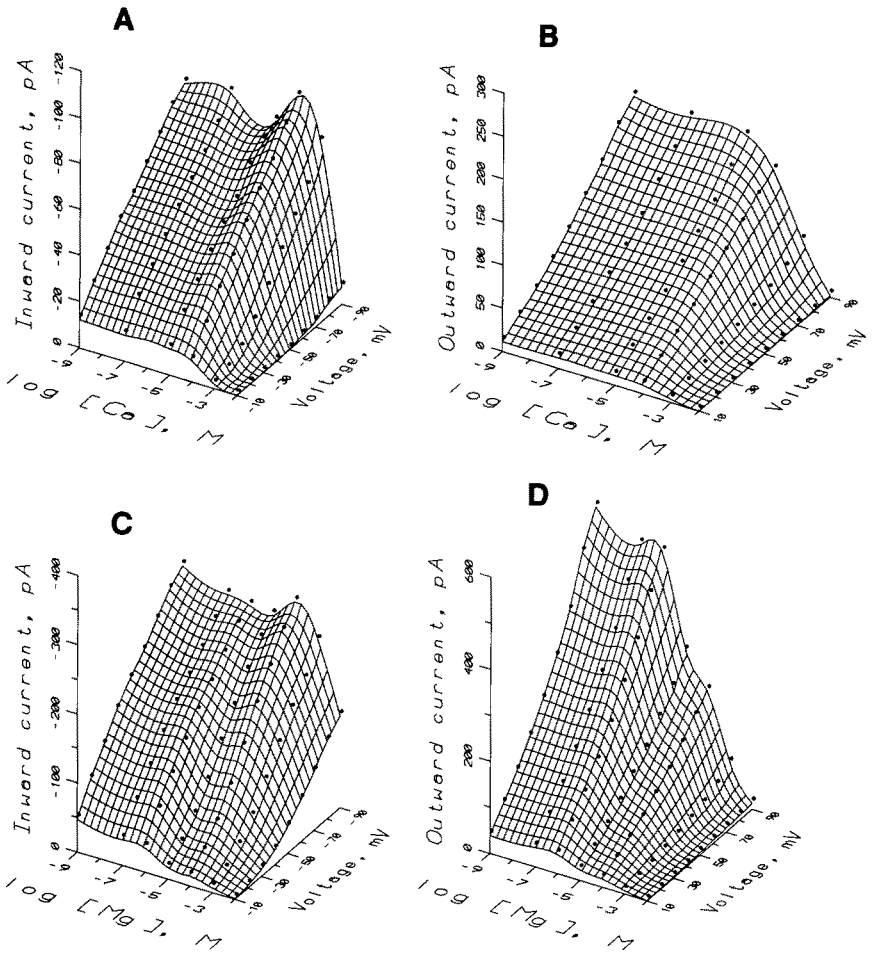


**Fig. 2.** Three-dimensional plots showing the effect of [Ca] (*A* and *B*) and [Mg] (*C* and *D*) at saturating cGMP levels. (*A*) Currents from the patch shown in Fig. 1 were digitally averaged in a 4-mV neighborhood every 10 mV and entered into Surfer® as described above. The left panel shows the inward currents recorded at potentials from −90 to −10 mV at 10-fold increases in the Ca concentration. The surface is essentially identical to the one computed using the enire data set, Fig. 1*B*. Multiple binding sites for Ca are suggested by the changes in the currents at low concentrations of Ca. From inspection, the midpoint for Ca block at −80 mV is ~2 mM Ca (*see* Table 1). Since the pipette is divalent free, the inward current is carried by sodium alone and block is occurring as Ca enters the channel from the bath. (*B*) The outward current surface shows little change in the current until $>10^{-5}$ M Ca where steep block begins. The midpoint for block of the outward current is ~.2 mM at 80 mV.

(*C* and *D*) A three-dimensional surface was constructed with the Surfer® program on data from a patch exposed to Mg as described above. As with the Ca surface, we see some changes in the current at low Mg levels and the low-affinity block is quite pronounced. Several features of this patch illustrate consistent differences between the effects of Ca and Mg. The inward current at high concentrations of divalents was more effectively blocked with Ca, whereas the outward current was more effectively blocked with Mg. Also, the outward currents were blocked by lower concentrations of Mg than Ca.

## Comparisons between the Effects of Ca and Mg at Saturating cGMP

Previous work (Tanaka & Furman, 1990; Colomartino et al., 1991; Zimmerman & Baylor, 1992) showed that the low-affinity Ca block of the cGMP channel is not specific for Ca. In particular, Mg was shown to produce a similar block of the inward current at mM concentrations. To investigate the divalent specificity of the high-affinity site, we replaced Ca with Mg and measured the *I-V* relations over the same concentration range.

In Fig. 2 we show the three-dimensional surfaces from a patch exposed to Ca (same patch as shown in Fig. 1) and another patch exposed to Mg. Fig. 2*A* and *C* are inward current surfaces and *B* and *D* are outward current surfaces. The Mg profile shows clearly the low-affinity binding site; changes in the current at very low Mg levels are not as pronounced as with Ca.

Several features consistently appeared with both Ca and Mg titration. First, the changes in the currents with divalent cations occurred over five to sixfold changes in the divalent concentrations; such

**Table 1.** Summary of $K_{0.5}$ values for Ca and Mg

| | | Low affinity | | Zimmerman & Baylor (1992) | |
|---|---|---|---|---|---|
| Divalent | [cGMP] | −80 mV | 80 mV | −30 mV | 30 mV |
| Ca ($n$ = 7) | 200 μM | 1 mM | 0.5 mM | 0.4 mM | 1.4 mM |
| Mg ($n$ = 9) | 200 μM | 10 mM | ~0.1 mM | 2.1 mM | 0.22 mM |
| Ca ($n$ = 6) | 20 μM | ND | ~1 mM | | |
| Mg ($n$ = 7) | 20 μM | ~1 μM | 1–10 μM | | |
| | | Voltage dependence at 200 μM cGMP | | | |
| Ca ($n$ = 8) | | 0.020 ± 0.0038 | 50 mV/decade | | |
| Mg ($n$ = 7) | | 0.016 ± 0.004 | 62 mV/decade | | |

effects were not expected from a single binding site model. Secondly, the reproducible changes in the current at low concentrations of divalents, between 10 and 100 nM, suggest the presence of a high-affinity binding site. Estimates of the concentration of divalents producing 50% block, the $K_{0.5}$ values, for the low-affinity site are given in Table 1.

Several features of the divalent effects also showed consistent differences between the divalents. First, Ca produced a more complete block of the inward current than Mg. One possible reason for the smaller inward currents with internal Ca is that Ca binds more tightly to the low-affinity site resulting in a longer transit time through the channel than Mg (or for inward currents, a longer dwell time in the channel) thereby occluding Na movement through the channels for a greater fraction of the time. Secondly, Mg block of the outward current was more complete than Ca block and was evident at lower concentrations than Ca block. Table 2 compares the averaged fraction of current in the presence of Ca and Mg. At 1 mM divalents, 55% of the inward current at −80 mV remains when Ca is present, as opposed to 84% when Mg is present. At 80 mV, the fraction of current remaining when 1 mM Ca or Mg was added was 24% for Ca but only 9% for Mg. The results of Colomartino et al. (1991) at 1 mM Ca and Mg are also shown in Table 2 and generally agree with our values. The general features of Ca and Mg block, shown in Fig. 2, were representative of >20 patches. Overall, the peak heights and valley depths varied from patch to patch, but the divalent locations of the peaks and valleys were remarkably constant.

**Table 2.** Comparison of the average fraction of the current remaining at 200 and 20 μM cGMP by Ca and Mg

| | −80 mV | 80 mV |
|---|---|---|
| 200 μM cGMP | | |
| 1 mM Ca ($n$ = 7) | 0.55 ± 0.22 | 0.24 ± 0.12 |
| 1 mM Mg ($n$ = 7) | 0.84 ± 0.13 | 0.09 ± 0.04 |
| 10 mM Ca | 0.34 ± 0.21 | 0.20 ± 0.24 |
| 10 mM Mg | 0.55 ± 0.15 | 0.06 ± 0.04 |
| 20 μM cGMP | | |
| 1 mM Ca ($n$ = 5) | 0.62 ± 0.48 | 0.20 ± 0.15 |
| 1 mM Mg ($n$ = 3) | 0.21 ± 0.20 | 0.02 ± 0.02 |
| 100 μM cGMP* @ −60 mV | | |
| 1 mM Ca | 0.66 | |
| 1 mM Mg | 0.60 | |
| 5 μM cGMP* @ −60 mV | | |
| 1 mM Ca | 0.44 | |
| 1 mM Mg | 0.34 | |

* Results taken from Colomartino et al. (1991).

### Changes in the *I-V* Relations at 20 μM cGMP as a Function of Calcium

The modest changes in cGMP-activated currents in the range of $10^{-9}$ to $10^{-5}$ M divalent concentrations were inconsistent with the large current changes we had seen in bilayer experiments when divalent levels were reduced to <150 μM (*see* Fig. 2, Tanaka et al., 1987, and *unpublished results*). In the patch experiments, we used saturating levels of cGMP to maximize the channel opening probability, whereas in the bilayer experiments, we used lower concentrations of cGMP to resolve individual channel fluctuations. To explore the effects of divalent cations at low levels of cGMP, we examined the currents over a wide divalent concentration range, using 20 μM cGMP to activate the channels. This nucleotide level is close to the $K_{0.5}$ for cGMP activation previously determined to be 24 μM (Tanaka et al., 1989), and much greater than the cytosolic levels, estimated in the dark as ~4 μM (Pugh & Lamb, 1990). The higher concentration was necessary to achieve a reasonable

signal to noise current ratio and for accurate current measurements in the presence of divalent block.

To determine the maximum current for each patch, *I-V* responses were measured at saturating cGMP without divalent cations. A control current was then recorded at 20 $\mu$M cGMP in the absence of divalent cations. With cGMP held constant at 20 $\mu$M, *I-V's* were generated as 10-fold increments of Ca were added at the cytoplasmic face of the patch. Results from one experiment are shown in Fig. 3. Panel *A* shows the typical, outwardly rectifying *I-V* at saturating cGMP. The *I-V* at 20 $\mu$M has a similar shape but the current is attenuated about 50%. When Ca was added to the bath at $10^{-8}$ M, the current decreased dramatically. The inward current is barely visible and the outward current is ~25% of the control value. Panel *B* is an expanded current axis revealing little change in the shape of the *I-V* from the 20 $\mu$M cGMP divalent-free control. When the $Ca_i$ level was raised to $10^{-7}$ M, the current increased modestly although it was still significantly smaller than the current at $10^{-9}$ M. Panel *C* shows the *I-V* relations at higher concentrations of Ca. As the Ca levels are increased, the *I-V* relations show appreciable shape changes for the currents in both directions.

As might be expected, much greater variability among patches was seen at low cGMP levels. Often the currents were noisy, especially at large hyperpolarizing potentials, and frequently the patches broke in high Ca solutions. The striking current attenuation at $10^{-8}$ M $Ca_i$, however, was very reproducible. A comparison of the effects of Ca and Mg at low cGMP levels is shown in the data from four separate patches in Fig. 4. Panels *A* and *C* show inward currents as $Ca_i$ is increased. The decrease in current at $10^{-8}$ M produces a deep valley in both surfaces. Panels *E* and *G* show similar depressions at the same concentration of $Mg_i$. In all patches, the currents rise as the divalent is increased above $10^{-8}$ M and local peaks are prominent in all panels. At even higher concentrations, the current decreases again but with more patch-to-patch variability. The outward currents, presented in the companion panels of Fig. 4, also show a prominent depression in the current at low divalent levels.

Data from multiple patches were averaged for each divalent and the normalized currents at −80 mV are plotted against the divalent concentration in Fig. 5. Despite the large variability shown by the standard deviations, the overall shapes of the averaged data agree with the features of the surfaces in Fig. 4. And while it may be more difficult to argue from the averaged data that the current rises above $10^{-8}$ M are significant, the large changes in the current at $10^{-8}$ M would not be predicted by a single low-affinity binding site.

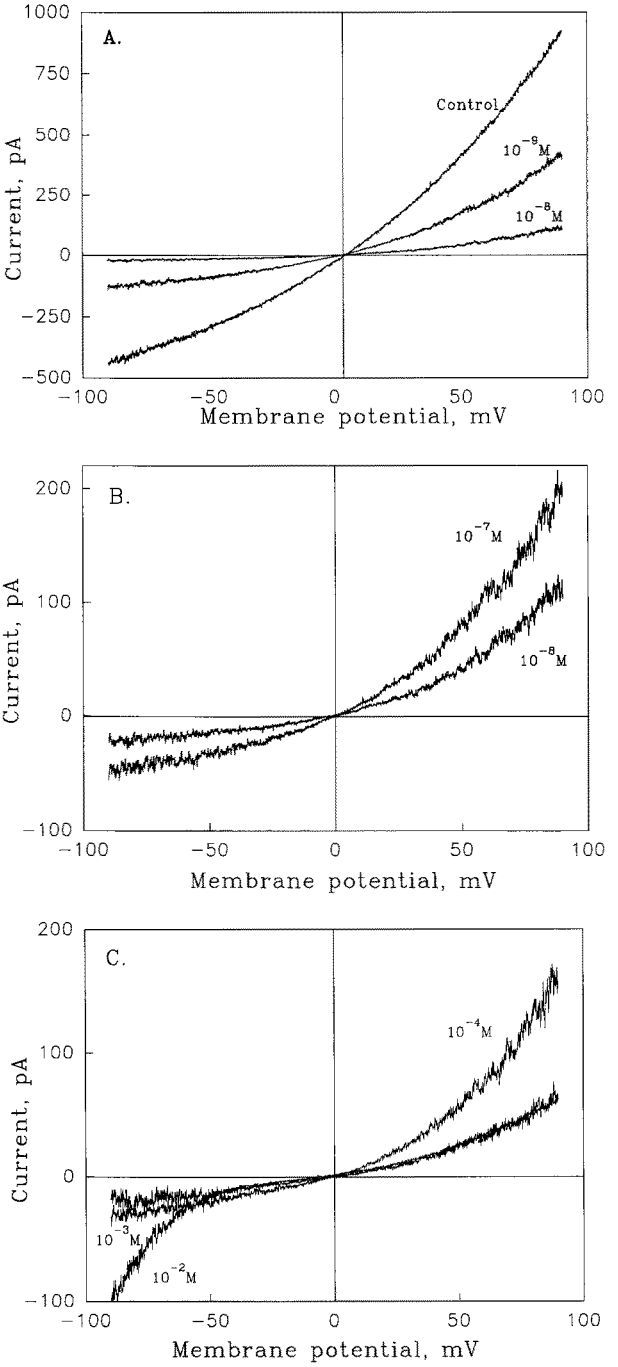


**Fig. 3.** The effect of Ca on currents activated by 20 $\mu$M cGMP (*A*) The net current in symmetrical solutions in the absence of divalent cations (Solution A) was recorded at 200 $\mu$M cGMP and 20 $\mu$M cGMP. The trace labeled $10^{-8}$M in *A* had 20 $\mu$M cGMP and $10^{-8}$ M Ca in the bath. The current decreased dramatically between $10^{-9}$ M Ca to $10^{-8}$ M Ca without an appreciable change in the shape. (*B*) The current at $10^{-7}$ M shows partial recovery from the block at $10^{-8}$ M. (*C*) *I-V* relations at $10^{-4}$ M, $10^{-3}$ M, and $10^{-2}$ M Ca. The current is significantly attenuated at 1 mM Ca. The inward current at 10 mM Ca, suggestive of a voltage-relieved block, probably reflects instability of the seal. In general, cells did not tolerate these conditions well and often broke during the strong depolarization in 10 mM Ca. (Patch 9327c1).

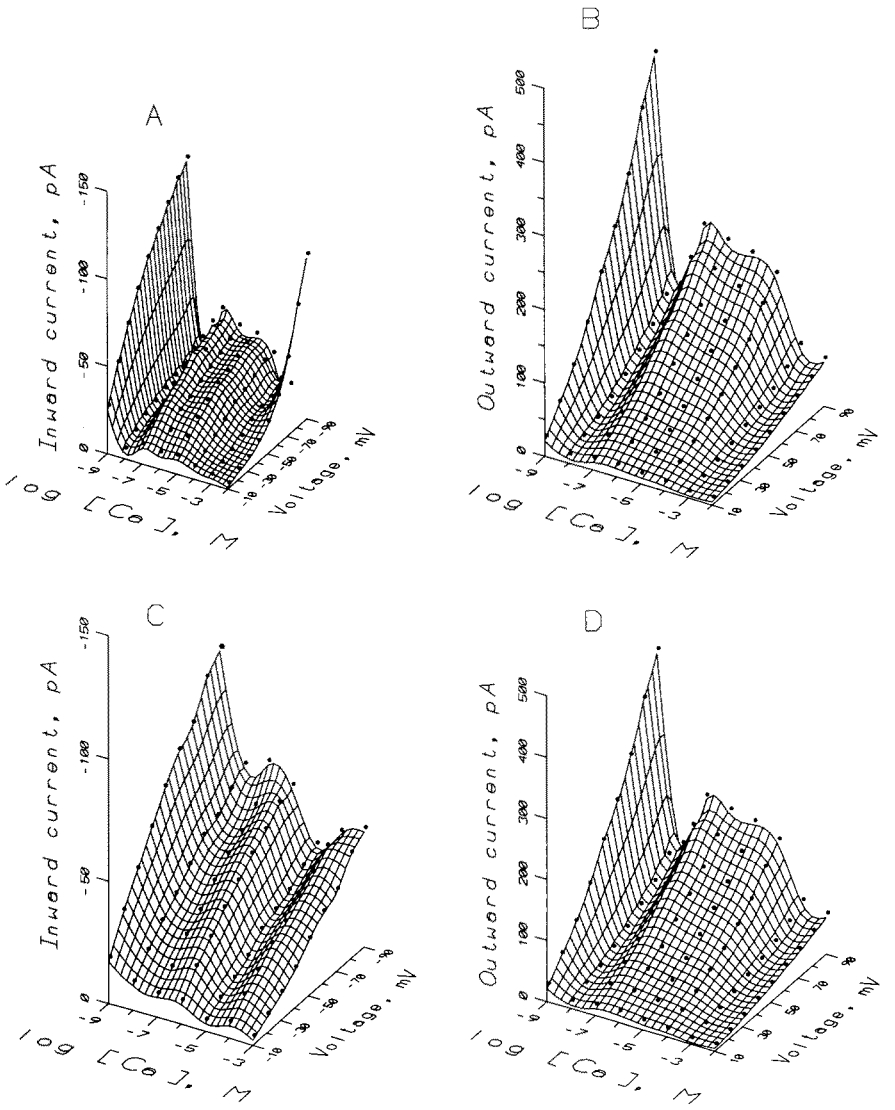


**Fig. 4.** Comparison of Ca and Mg effects in 20 $\mu$M cGMP. (*A–D*) Three-dimensional profiles for two patches exposed to Ca; (*E–H*) show surfaces from two patches exposed to Mg. The large decrease in the current seen at $10^{-8}$ M Ca in Fig. 3 appears as a deep valley in the surfaces of both inward and outward currents in all patches. The currents show partial recovery at ~1 $\mu$M divalents. Surfaces were constructed as described in Fig. 3. As the Ca is raised from $10^{-9}$ M to $10^{-8}$ M, both inward and outward currents decrease to 10 or 20% of the initial current. (Patch 9327c1, Ca: Patch 9325c2 and 9325c1, Mg). The initial block for both Ca and Mg occurs at $10^{-8}$ M and appears to block currents in both directions. The lower-affinity block, occurring between $10^{-5}$ and $10^{-4}$ M for Mg but not until $10^{-3}$ M for Ca, is the most distinguishing difference between the two divalents. Average values of the midpoints for low-affinity block are given in Table 1.

The current block at low levels of cGMP are compared with results on similar experiments by Colomartino et al. (1991) using 5 $\mu$M cGMP in Table 2. The fraction of inward current at −80 mV with 20 $\mu$M cGMP was 62% with 1 mM Ca and 21% with 1 mM Mg. At 5 $\mu$M, Colomartino et al. reported 44% of the control current with 1 mM Ca and 34% with 1 mM Mg. In both cases, the fraction of current blocked with 1 mM divalent cations is significantly different from that fraction blocked at high cGMP levels.

## Voltage Dependence of Divalent Effects

The voltage dependence of block provides information on the affinity and relative locations of the blocking site within the transmembrane field for the simple case of an impermeant ion reacting with a single binding site (Woodhull, 1973). The Woodhull derivation cannot be applied to Ca block of the photoreceptor channel since several of the initial assumptions are violated in this situation. However, we can use the voltage dependence of the divalent effects to qualitatively decide whether the divalent sites are located inside or outside of the membrane field.

In Fig. 6, a semi-log plot of divalent block *vs.* voltage is shown for data at high and low concentrations of cGMP. At saturating cGMP levels, Fig. 6*A*, no voltage dependence of the inward current block is seen at low levels of Ca suggesting that the divalent site lies outside the membrane field. At 1 and 10 mM, the voltage dependence is 50 mV/decade and 38 mV/decade, respectively, suggesting that the low-affinity site lies within the membrane field. For outward

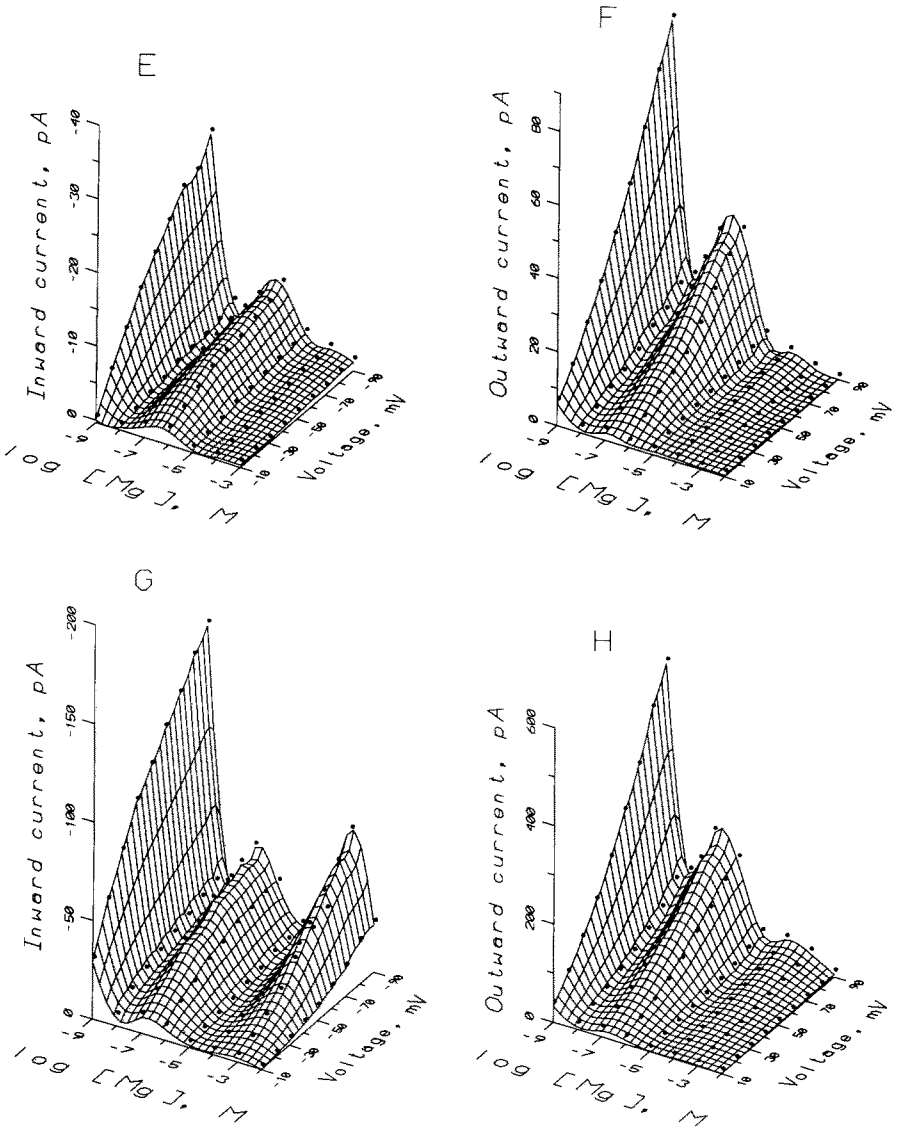


**Fig. 4.** *Continued*

currents, the divalent block of current is independent of voltage, consistent with divalent, as well as monovalent, permeation through the channel. The voltage dependence of the low-affinity divalent block of the inward current was averaged for several patches and the averaged values are given in Table 1.

Fig. 6*B* shows the voltage dependence of Mg block at 20 $\mu$M cGMP. As seen in Fig. 6*A*, the voltage dependence of block is slight at low Mg concentrations. At higher concentrations of Mg, voltage dependent inward block is observable with slopes (*see* figure legend for the range over which slopes were determined) of 63 and 50 mV/decade for 1 and 10 mM Mg, respectively.

Our estimates of the concentration and voltage dependence of block for the low-affinity site are in good agreement with the estimates of Zimmerman and Baylor (1992). Average values from their work, measured at ±30 mV, are compared with our measurements at ±80 mV in Table 1.

## Discussion

These experiments provide the first evidence for a voltage-independent, high-affinity Ca binding site at the cytoplasmic face of the nucleotide-activated photoreceptor channel. Reducing cGMP levels greatly enhances the effects of Ca on macroscopic currents. At 20 $\mu$M cGMP, changes in cytoplasmic Ca levels near the range of Ca signaling in the cell, produce a 5 to 10-fold change in the macroscopic currents. The presence of a divalent binding site

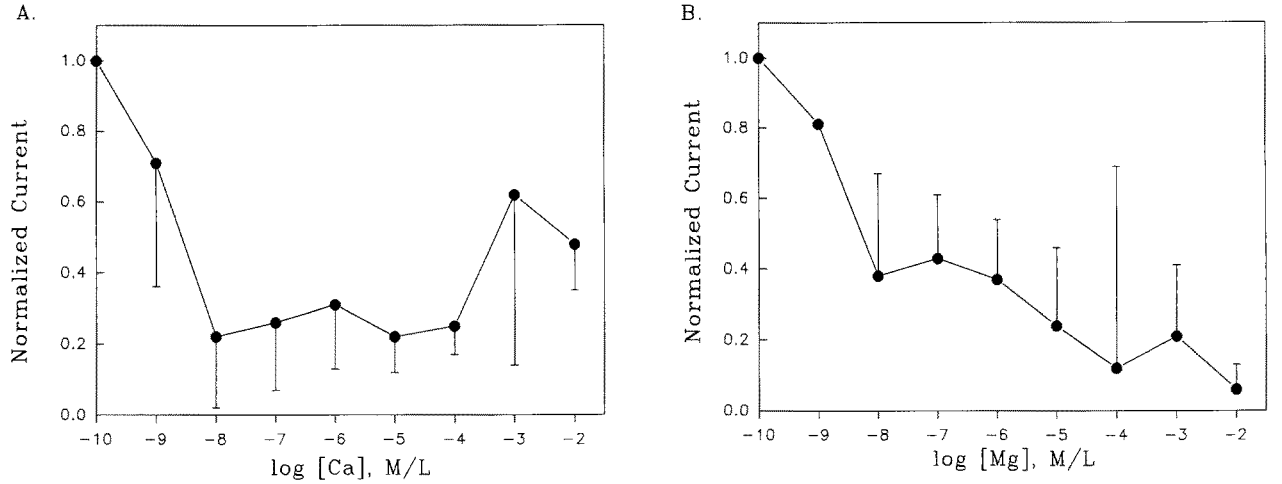


**Fig. 5.** Averaged effects of Ca and Mg at low cGMP levels. Data with standard deviations about the mean were averaged from seven patches at −80 mV for Ca (*A*) and Mg (*B*) although not all concentrations were available for each patch. As the divalent concentration is raised from $10^{-9}$ M, the mean inward current is reduced to ~20% in $10^{-8}$ M Ca and 40% at $10^{-8}$ M Mg. With further increase in the divalent concentrations, the currents recover somewhat. Variability among the patches is considerable and contributes to the large deviations; however, the same general features seen in the three-dimensional surfaces are also clear in these data.

modulated by cytosolic Ca at physiological concentrations raises several questions. Does the Ca site affect ion permeation directly or indirectly by alterations in the channel kinetics? Does this binding site play a physiological role in photoreceptor signaling?

## The Effects of Divalent Cations on Macroscopic Patch Currents

Zimmerman and Baylor (1992) recently examined the interactions of Na, Ca and Mg in excised patches to better understand ion permeation through the cGMP-activated channel. They developed a single binding site permeation model to explain a number of experimental results involving the physiological ions. Based on their model, they conclude that a single, low-affinity binding site dominates ion permeation and block in the photoreceptor channel although other sites, such as a high-affinity site, may be present.

Zimmerman and Baylor fitted their conductance *vs.* divalent concentration data under conditions where we see little effect of the high-affinity site, i.e., at saturating levels of cGMP and ±30 mV (*see* their Figs. 7 and 8). While we have tried to fit our *I-V* relations at 200 μM cGMP with a single-site model similar to the one used by Zimmerman and Baylor (*results not shown*), our efforts have failed to predict the current changes at low levels of divalent cations and at greater voltages (−90 mV). This might be expected if the high-affinity site affects channel gating rather than permeation. In view of the multiple conducting states of the channel (Zimmerman & Baylor, 1986; Ildefonse & Bennett, 1991), a permeation model based on data at saturating cGMP levels may only describe the highest conducting state of the channel that may be dominated by the low-affinity site. The permeation features of the other conducting states, open more frequently at lower nucleotide levels, may vary in their selectivity properties as suggested by Cervetto et al. (1988).

Colomartino et al. (1991) examined the effects of divalent cations at high and low levels of cGMP and concluded that both divalent block and permeation depend on the level of cGMP. When they compared the blocking effect of 1 mM Ca and Mg at different concentrations of cGMP, they found that the fraction of current blocked was dependent on the nucleotide concentration in a complex way. Our results show a similar complex interaction between block and nucleotide activation (*see* Table 2). Colomartino and collaborators also noted that Mg levels, but not Ca levels, affected the cGMP dose-response relationship suggesting a difference between the divalents in their interaction with channel gating. They proposed that different conducting states of the channel have different affinities for the divalent cations. The authors note that besides the low-affinity, voltage-dependent divalent blocking site, divalent cations can block the channel in a voltage-independent way. This observation matches the lack of voltage dependence we see for the high-affinity site.

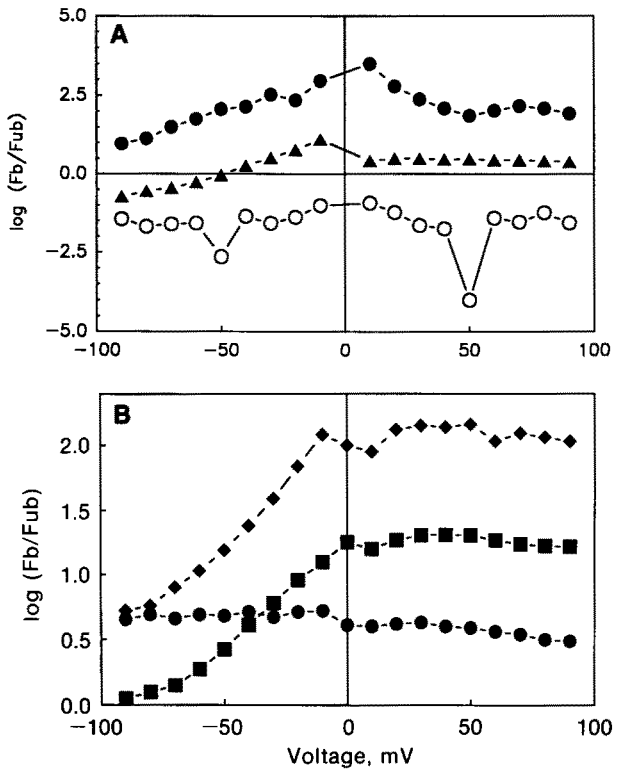


**Fig. 6.** Fraction of current blocked *vs.* $V_m$. (*A*) Block at 200 $\mu$M cGMP for Ca. The fraction of current blocked ($F_b$) by either $10^{-7}$ M (○), 1 mM (▲) or 10 mM (●) Ca was calculated for the patch shown in Fig. 1. The slope of log (Fraction blocked/Fraction unblocked) ($F_b/F_{ub}$) *vs.* $V_m$ was fitted for each concentration. At $10^{-7}$ M Ca, the slope, determined from a linear fit from −90 to −10 mV (omitting the value at −50 mV), was 0.005 ($r$ = 0.664, $n$ = 8). At higher [Ca], slopes were determined from −90 to −30 mV; the slope at 1 mM Ca is 0.02 ($r$ = 0.99) and the slope at 10 mM Ca is 0.026 ($r$ = 0.99). These slopes correspond to 50 mV and 38 mV/decade, respectively. (*B*) Voltage dependence of Mg block at 20 $\mu$M cGMP at 10 nM (●), 1 mM (■) and 10 mM (◆). No voltage dependence is seen in the block at 10 nM Mg. At 1 mM Mg, the slope was 0.016 from −70 to −10 mV (62 mV/decade). At 10 mM Mg, the slope was 0.020 over the same voltage range which is 38 mV/decade. (Patch 9325c2).

### Physiological Relevance of the High-Affinity Site

Our results showing the modulation of cGMP-activated currents by a high-affinity divalent binding site and the complex interactions between divalent and nucleotide levels seen by Colomartino et al. (1991) raise the possibility that cytosolic Ca levels feedback on the channel directly to regulate the current. Given the small excursion in intracellular Ca levels, estimated from 140 to 220 nM (Ratto et al., 1988), and the $>10^3$-fold change in light sensitivity with changes in background light levels (Baylor et al., 1980), it seems reasonable to expect multiple points of Ca feedback in the outer segment.

To investigate the cellular role of the high-affinity site, it will be necessary to develop a better understanding of channel permeation and block, ionic selectivity, and nucleotide gating. The physiological conditions under which the channel functions imply a competition between Na, Ca and Mg at each membrane face, adding considerable complexity to determining the flux of each ion in the macroscopic currents. In addition, for conditions reflective of the cytoplasmic environment, the level of cGMP should be reduced to dark levels, estimated to be ~4 $\mu$M (Pugh & Lamb, 1990). Ultimately, we seek to answer physiologically relevant questions about the channel such as what fraction of the photoreceptor current is carried by Ca and how does the fraction change as background light levels change. Similar questions have been addressed in other channels where relative Ca entry is important. Decker and Dani (1990) recently developed a permeation model for the acetylcholine receptor that predicts the fraction of current carried by both Na and Ca under physiological conditions. Although the cGMP-activated channel gating and permeation appear more complex, models of this type should be a useful starting point in predicting Ca entry in the outer segment.

## Conclusion

Recent work on the cGMP-activated channel shows that both channel activation and permeation are more complex and interrelated than initially appreciated. Whether this complexity plays a direct role in physiological signaling or an indirect, supporting role subserving physical and structural needs of the channel monomers to form the channel complex, is unclear at present. Given the photoreceptor's efforts to regulate intracellular Ca levels, it would seem likely that all these findings hint at important, but subtle, controls for Ca entry into the OS.

The authors thank Drs. Kim Cooper, Bob French and Gregg Wells for helpful discussions of channel selectivity.

This work was supported by NIH Grants EY-06640, BRSG 07083-21, and 05415-25 to J.C.T., and EY01583 Core support.

## References

Baylor, D.A., Matthews, G., Yau, K.-W. 1980. Two components of electrical dark noise in toad retinal rod outer segments. *J. Physiol.* **309**:591–621

Briggs, I.C. 1974. Machine contouring using minimum curvature. *Geophysics* **39**:39–48

Cervetto, L., Menini, A., Rispoli, G., Torre, V. 1988. The modulation of the ionic selectivity of the light-sensitive current in isolated rods of the tiger salamander. *J. Physiol.* **406**:181–198

Colomartino, G., Menini, A., Torre, V. 1991. Blockage and permeation of divalent cations through the cyclic GMP-activated channel from tiger salamander retinal rods. *J. Physiol.* **440**:189–206

Decker, E.R., Dani, J.A. 1990. Calcium permeability of the nicotinic acetylcholine receptor: The single-channel calcium influx is significant. *J. Neurosci.* **10**:3413–3420

Fabiato, A., Fabiato, F. 1979. Calculator programs for multiple metals and ligands. *J. Physiol. (Paris)* **75**:463–505

Furman, R.E., Tanaka, J.C. 1988. Patch electrode glass composition affects ion channel currents. *Biophys. J.* **53**:287–292

Furman, R.E., Tanaka, J.C. 1990. Monovalent selectivity of the cyclic guanosine monophosphate-activated ion channel. *J. Gen. Physiol.* **96**:57–82

Hamill, O.P., Marty, A., Neher, E., Sakmann, B., Sigworth, F. 1981. Improved patch-clamp techniques for high-resolution current recording from cells and cell-free membrane patches. *Pfluegers Arch.* **391**:85–100

Ildefonse, M., Bennett, N. 1991. Single channel incorporation of native vesicles into planar bilayers. *J. Membrane Biol.* **123**:133–147

Kantrowitz-Gordon, W.E., Zimmerman, A.L. 1991. Long-term changes in the cGMP-activated conductance in excised patches from rod outer segments. *Biophys. J.* **59**:533*a*

Karpen, J.W., Zimmerman, A.L., Stryer, L., Baylor, D.A. 1988. Gating kinetics of the cyclic-GMP-activated channel of retinal rods: Flash photolysis and voltage-jump studies. *Proc. Natl. Acad. Sci. USA* **85**:1287–1291

Liebman, P.A., Parker, K.R., Dratz, E.A. 1987. The molecular mechanism of visual excitation and its relation to the structure and composition of the rod outer segment. *Annu. Rev. Physiol.* **49**:765–791

Martell, A.E., Smith, R.M. 1974. Critical Stability Constants. Vol. 1: Amino Acids. Plenum, New York and London

Menini, A. 1990. Currents carried by monovalent cations through cyclic GMP-activated channels in excised patches from salamander rods. *J. Physiol.* **424**:167–185

Pugh, E.N., Lamb, T.D. 1990. Cyclic GMP and calcium: the internal messengers of excitation and adaptation in vertebrate photoreceptors. *Vision Res.* **30**:1923–1948

Ratto, G.M., Payne, R., Owen, W.G., Tsien, R.Y. 1988. The concentration of cytosolic free calcium in vertebrate rod outer segments measured with Fura-2. *J. Neurosci.* **8**:3240–3246

Su, K., Furman, R.E., Tanaka, J.C. 1991. Evidence for 2 calcium binding sites in cGMP-activated channels. *Biophys. J.* **59**:407*a*

Tanaka, J.C., Eccleston, J.F., Furman, R.E. 1989. Photoreceptor channel activation by nucleotide derivatives. *Biochemistry* **28**:2776–2784

Tanaka, J.C., Furman, R.E. 1990. Divalent cation effects on cGMP-activated sodium currents in photoreceptor patches. *Biophys. J.***57**:319*a*

Tanaka, J.C., Furman, R.E., Cobbs, W.H., Mueller, P. 1987. Incorporation of a retinal rod cGMP-dependent conductance into planar bilayers. *Proc. Natl. Acad. Sci. USA* **84**:724–728

Yau, K.-W. 1991. Calcium and light adaptation in retinal photoreceptors. *Curr. Op. Neurobiol.* **1**:252–257

Yau, K.-W., Baylor, D.A. 1989. Cyclic GMP-activated conductance of retinal photoreceptor cells. *Annu. Rev. Neurosci.* **12**:289–327

Woodhull, A.M. 1973. Ionic blockage of sodium channels in nerve. *J. Gen. Physiol.* **61**:687–708

Zimmerman, A.L., Baylor, D.A. 1986. Cyclic GMP-sensitive conductance of retinal rods consists of aqueous pores. *Nature* **321**:70–72

Zimmerman, A.L., Baylor, D.A. 1992. Cation interactions within the cyclic GMP-activated channel of retinal rods from the tiger salamander. *J. Physiol.* **449**:759–783

Received 10 July 1992; revised 28 September 1992